Computational Biology and Chemistry 74 (2018) 49–62

Contents lists available at ScienceDirect

Computational Biology and Chemistry

journal homepage: www.elsevier.com/locate/compbiolchem

Design and screening of syringic acid analogues as BAX activators-An *in silico* approach to discover "BH3 mimetics"

Srinivasulu Cheemanapalli[a,*], Anuradha C.M.[b], Suresh Babu Pakala[c], Suresh Kumar Chitta[a]

[a] Department of Biochemistry, DBT-Bioinformatics Infrastructure Facility, Sri Krishnadevaraya University, Anantapuramu, 515 003, A.P., India
[b] Department of Biotechnology, Sri Krishnadevaraya University, Anantapuramu, 515 003, A.P., India
[c] Department of Biology, Indian Institute of Science Education and Research (IISER), Tirupathi, 517 507, A.P., India

ARTICLE INFO

Article history:
Received 1 September 2017
Received in revised form 29 January 2018
Accepted 5 March 2018
Available online xxx

Keywords:
Apoptosis
BAM-7
Syringic acid
Docking
Mutation
ProSA-web

ABSTRACT

Although BAX, which is a molecular hit squad that incentive apoptosis was found to be an attractive emerging target for anticancer agents. The molecular mechanism of small molecules/peptides involved in the BAX activation was remain unknown. The present focus of the study is to identification and development of novel molecules which are precisely activates BAX mediated apoptosis. In this process we identified some syringic acid analogues associated with the BAX hydrophobic groove by a virtual-screen approach. Results from the docking studies revealed that, SA1, SA9, SA10, SA14 and SA21 analogues have shown good interaction with BAX trigger site, of which SA10 and SA14 bound specifically with Lys21 at α1 helix of BAX, a critical residue involved in BAX activation. All docking calculations of SA analogues were compared with clinically tested BH3 mimetics. In this entire *in silico* study, SA analogous have performed an ideal binding interactions with BAX compared to BH3 mimetics. Further, *in silico* point mutation of BAX-Lys21 to Glu21 resulted in structural change in BAX and showed reduced binding energy and hydrogen bond interactions of the selected ligands. Based on these findings, we propose that virtual screening and mutation analysis of BAX is found to be the critical advance method towards the discovery of novel anticancer therapeutics.

1. Introduction

BAX is a pro-apoptotic BCL-2 family member that executes the apoptosis through mitochondrial pathway (Gavathiotis et al., 2010). The relative levels of pro and anti-apoptotic proteins in the cell determine the sensitivity of apoptotic event during a stimuli and the resistance in apoptosis can be due to the excess levels of anti-apoptotic proteins in the cell (Nuessler et al., 1999; Sawada et al., 2000). Structural analysis of BAX/BIM BH3 complex described that; a new binding site is located at N-terminal site formed by the helix1 and 6 of the BAX protein that engage its activation (Gavathiotis et al., 2012). Exposed form of BAX activation requires the major conformational changes prompted by the conversion of α1-α2 loop from closed conformation to open form (Gavathiotis et al., 2008). BIM SAHB-BAX interaction was carried out through NMR analysis, which identifies the minor changes of loop residues located between H1 and H2 of BAX (Gavathiotis et al., 2008; Vogler et al., 2009). Identification of small molecules that mimics the function of BIM BH3 peptide, is one of the strategy for the activation of pro-apoptotic Bcl-2 members (Nguyen et al., 2007; Wang et al., 2006). BAX activity neutralized by their counterparts i.e. anti-apoptotic Bcl-2 proteins; however, in majority of cancer cells, BAX is the most functional protein and it could be an effective drug target for the cancer treatment (Walensky and Gavathiotis, 2011; Lessene et al., 2008; Baell and Huang, 2002).

Several chemotherapeutic agents or knockdown of certain cell cycle proteins can induce the BAX-dependent apoptosis in cancer cells (Zheng et al., 2018). Earlier investigations found that, the natural plant-derived Gossypol and its derivatives showed antitumor activity in *in vitro* and animal models by modulating the BCL-2 members via its BH3 mimetic properties (Azmi et al., 2011; Quinn et al., 2011a, 2011b; Wilson et al., 2010). BTSA1, a pharmacologically optimized BAX activator that potently and specifically binds with the BAX trigger site and induced conformational changes of BAX leading to BAX mediated apoptosis in leukemia cell lines (Reyna et al., 2017). Other findings suggested

* Corresponding authors.
E-mail addresses: srenubio@gmail.com (S. Cheemanapalli), dr.cm.anuradha@gmail.com (A. C.M.), pakalasb@iisertirupati.ac.in (S.B. Pakala), suresh.chitta@skuniversity.ac.in (S.K. Chitta).

https://doi.org/10.1016/j.compbiolchem.2018.03.003
1476-9271/

that proapoptotic activity of BAX also can regulate by S184 phosphorylation site located in hydrophobic C-terminal tail of BAX. SMBA1, SMBA2 and SMBA3 are the small-molecule which can induce conformational changes in BAX by blocking S184 phosphorylation (Xin et al., 2014). Syringic acid (SA), a phenolic compound derived from edible plants and fruits (Ramachandran and Raja, 2010) bring its anti-cancer activity through inducing cell-cycle arrest, apoptosis, decreasing invasion, cell migration and prevents the NFkB-DNA binding activity (Abaza et al., 2013). SA exhibits antiangiogenesis activity by down regulation of VEGF expression in Zebra fish embryos (Karthik et al., 2014). Virtually derived SA analogues shown to inhibit proteasome activity in human malignant melanoma cells (Orabi et al., 2013). Some hydrazones derived from SA have shown potent free radicle scavenging activity by inhibition of ROS generated in diseased cell (Belkheiri et al., 2010). Design and screening of small molecules with different chemical moieties capable of targeting Bcl-2 family proteins are of great therapeutic interest (Azmi et al., 2011; Kazi et al., 2011; Delgado-Soler et al., 2012; LaBelle et al., 2012).

Therapeutic strategies to selectively activate apoptosis in cancer have focused on inhibiting anti-apoptotic BCL-2 proteins. In the present study, we designed several analogues of SA and screened for their druggability, toxicity and binding affinity with BAX protein using *in silico* method. Only few selected compounds were further docked with BAX trigger site for the investigation of BH3 mimetics by observing the binding mode of standard BAX activator (BAM-7). The *in silico* point mutation of BAX was developed using pyMOL mutagenesis wizard, which impaired the binding strategy and geometry of active site for the ligands examined in the present study. These are clearly explained by changes in ProSA web Z values and electrostatic potential energy of native and mutant models. Based on these *in silico* analysis, first time we have reported some SA analogues that selectively binds to BAX trigger site, as evident from the *in silico* mutation and docking studies. This study provides insights for the development of BH3 mimetics/direct BAX activators which can induce the BAX mediated apoptosis in cancer cells.

2. Materials and methods

2.1. Data set preparation

A series of SA analogues were prepared by inducing structural modifications onto the source structure using the database of substituents and linkers available in Molinspiration server (Lipinski et al., 2001). These were designed by maintaining the synthetic procedure. A data set of 563 SA analogues were drawn by Chem Draw ultra 8.0 (Cambridge Soft, Cambridge, MA, USA) and all the generated structures were simulated by Hyper Chem as described elsewhere (http://www.hyper.com, 2003).

2.2. Virtual Screening and Drug-Likeness PredictionVirtual screening and drug-likeness prediction

Virtual screening of chemical database is a supportive approach to identify novel and potential leads which are suitable for further optimization. In this study, the *in silico* physicochemical properties of all designed SA analogues were predicted according to the Lipinski's Rule of Five (Lipinski et al., 1997) using the molinspiration software. This data predicted the desired ranges of physiochemical properties for newer molecules and they were used as filters for drug development.

2.3. ADMET prediction

The filtered hits were further screened by ADMET properties which refer to the adsorption, distribution, metabolism, excretion and toxicity of a molecule within an organism. ADMET properties of the novel compounds were calculated using the pre-ADMET server (http://preadmet.bmdrc.org/) (Irvine et al., 1999; Zhao et al., 2001).The ADMET properties of *in vitro* plasma protein binding, *in vitro* MDCK cell permeability, human intestinal absorption, *in vivo* BBB penetration and *in vitro* Caco-2 cell permeability were predicted using this server. Finally, the compounds, which passed the above various filters, were subjected to molecular docking studies and visual inspection. Among all designed analogues, 29 compounds include SA were chosen for docking on to BAX trigger site based on their ability to follow Lipinski rule of five and ADMET properties.

2.4. Molecular docking

The SA based structural analogues were used for virtual screening against the selected active site of the BAX protein to understand their molecular interaction and binding mode by docking analysis. The docking studies were carried out with an automated docking program Auto Dock4.2 (Morris et al., 2009). Before docking all the components such as BAX, SA, and its analogues were optimized. BAM-7 and other previously characterized BH3 mimetics are used as reference compounds for comparative docking analysis.

2.4.1. Protein and ligand preparation

The crystal structure of BAX (PDB: 1F16) was obtained from NMR structure in Protein Data Bank (Berman et al., 2002). Prior to initiating the docking simulations, all non-protein molecules were removed, for any alternative atoms locations only the required location was retained. The 3D structures of the SA and its designed analogues were generated by PRODRG server (Schuettelkopf and Van Aalten, 2004) and pre-optimized using the MMFF94x force field. 3D structures of reference compounds (BH3 mimetics) were retrieved from Pubchem database. All ligand molecules were docked against energy minimized BAX using Auto Dock4.2 docking program.

2.4.2. Prediction of BAX active site residues

The structural and binding site information of BAX was analyzed through PDBSum (http://www.ebi.ac.uk/pdbsum) and is linked to Computed Atlas of Surface Topography of Proteins (CASTp) program (http://cast.engr.uic.edu). The confluence of α-helices 1 and 6 formed the BH3 trigger site on BAX and is structurally defined by a hydrophobic groove comprising the amino acids Met20, Ala24, Leu27, Ile31, Ile133, Met137 and Leu141 and a perimeter of charged and hydrophilic residues, including Lys21, Gln28, Gln32, Glu131 and Arg134.

2.4.3. Docking method

Protein-ligand docking method employed to understand the binding interaction of SA analogues onto BAX protein. The complete docking protocol was followed according to method described by Cheemanapalli et al., 2016. The hierarchies of ranking positions for docked ligands are assigning based on lowest binding energies (Kcal/mol). The higher negative value of docking score indicates a greater binding affinity of the ligand with receptor. After docking, the ligand-receptor complexes were analyzed by PyMOL visualizing program (Delano, 2006).

2.5. In silico *point mutation of BAX*

For understanding the significance of binding efficiency of BAX with selected ligands, we performed the single amino acid substitution in the α1 helix of its trigger site. The BH3-induced BAX activation and binding of BIM SAHB to BAX can be weakened

by K21E point mutation (Gavathiotis et al., 2010). *In silico* point mutation of Lys21 to Glu21was generated using the mutagenesis tool in pyMOL and energy minimization of the mutated protein is performed using Swiss PDB Viewer (Thompson et al., 1994). The energy minimized mutant protein is used for further docking studies. In the pyMOL mutagenesis, the replaced residues with best side chain conformer (rotamer) fits to the protein structure is selected and exported as pdb file. The quality of mutant protein was checked by Verify3D (Luthy et al., 1992; Bowie et al., 1991) and ProSA-web (Sippl, 1993) tools. Verify 3D calculates the position of amino acid residues and its environmental score in the 3D models. The mutation creates any structural problems can be identified by the comparison of scores of mutated amino acid residues with wild type residues. ProSA-web calculates the Z-score (energy profile) for overall model quality and energy deviation of the protein. Experimentally determined all protein chains in PDB are displayed in the Z-score plot and it is used for the better understanding for the prediction of Z-score of specific model. If the Z-score is outside the range of native proteins, the model structure is predicted to be as an error. The surface potential energy shows the changes in charge distribution and amino acid residue content in the protein. The charge distribution on the protein surface represented in different colors; the blue color represents the electropositive potentials, red color represents the electronegative potentials whereas the green represents a potential halfway between the electropositive and electronegative extremes. Amino acid mutations alter the protein flexibility as well as intra-or intermolecular hydrogen bonding network, resulting in significant deviation away from the wild-type characteristics of the proteins.

3. Results and discussion

Exploring the novel anti-cancer agents extracted from natural sources or synthetic procedures have become a significant strategy in cancer therapy. Moreover, to identify the selective therapeutic agents which precisely induce the apoptosis through BAX activation, a need to develop potent drug-like molecules. Currently, several BH3 mimetics are developed and most of them are under clinical trials. For the development of an effective BH3 mimetics, we interested to work on a small molecule, syringic acid. While it has been shown several therapeutic applications, it has an ability to inhibit the carcinogenesis. In the present study we designed a library of SA analogues and screened for their property of BH3 mimetic through docking analysis. SA analogues were designed by a series of structural changes induced on SA main structure by using Molinspiration server. All the designed molecules were further screened by subjecting through Lipinski's rule and ADMET tools. The molecules were filtered based on their druglike ness and ADME properties. The finally selected molecules were screened for their BH3 mimetic action through docking studies. In docking analysis, all ligand molecules were docked on energy minimized BAX protein using Auto Dock4.2. The grid based energy evaluates the ligand conformation in docking simulations. The ligands placed in auto grid covered grid map dimensions 60 Å × 60 Å × 60 Å with grid spacing of 0.375 Å. The docking protocols Lamarckian Genetic Algorithm (LGA), Genetic Algorithm (GA), and simulated annealing are implemented in the Auto Dock4.2 for the calculation of ligand binding conformations. In all the docking simulations the population size and docking runs were set to 300 and 100 respectively. Additional docking parameters were set to default values for all the other three algorithms. The outcomes of docking results were ranked by the binding energy (kcal/mol) and inhibition constants (Ki). The conformation of each docked compound obtained based on the criterion of from 2.0 Å root mean square deviation (RMSD) using Auto Dock cluster module. For the comparison of binding properties of SA analogues, we used clinically tested BH3 mimetics as a reference compounds in this docking analysis.

3.1. Design and virtual screening of SA analogues

The present focus of the study is to design a set of SA analogues and screen for their druggability, ADMET properties and finally access their binding interaction with BAX target protein using an *in silico* approach. Among all, 29 compounds were chosen for docking onto BAX based on their ability to follow Lipinski rule of five and ADMET properties. The physicochemical properties such as TPSA (Polar surface area), molecular weight, logP (Octanol-water partition coefficient), H-bond donors/acceptors and number of rotatable bonds of the selected compounds calculated *in silico* are summarized in Table S1. The results showed that all the screened analogues were satisfied the Lipinski's rule.

3.2. ADMET predictions

ADME analysis of 55 compounds (SA and its 54analogues) predicted for their Absorption, Distribution, Metabolism and Excretion through Pre-ADMET software. The druggability of the designed compounds should have the perfect ADME properties, and only they will be approved as a drug in clinical tests. In the present study, out of 55compounds, 29 were shown satisfactory ADMET results (Table S2). All 29 compounds showed well intestinal absorption and middle permeability for *in vitro* Caco-2 cells. The pharmacodynamics and pharmacokinetic properties of a drug can influence by the degree of binding to plasma proteins. The bound drug in plasma can serve as a reservoir for free drug removed by various elimination processes thus prolonging the duration of action. The Extensive plasma protein binding will increase the amount of drug that has to be absorbed before effective therapeutic levels of unbound drug are reached. Here, in with respect to ADME, the percent of drug bound with plasma proteins was predicted and the compounds SA3, SA9, SA11, SA14, SA29, SA36, SA37, SA46 and SA49 were predicted to bind strongly and remaining compounds were weakly bound to plasma proteins. The compounds SA1, SA14, SA21, SA36, and SA37 showed low permeability and the rest of them showing middle permeability for *in vitro* MDCK cells. The effective delivery of drugs to the CNS can be determined by BBB. For *in vivo* blood brain barrier penetration, the compounds SA1, SA3, SA12, SA14, and SA52 showed poor absorption and the remaining all showed middle absorption to CNS. Only the CNS active compounds must pass across the BBB and avoid the side effects caused by CNS inactive drugs.

3.3. Docking study

The BAX protein consisted of 192 residues with 9α helices without β sheets. The N-terminal BH3 trigger site on BAX is formed by the confluence of α-helices 1 and 6 (Fig. 1A) and the binding mode of SA and its analogues on the trigger site was illustrated in Fig. 1B. Molecular docking studies of compounds against BAX trigger site revealed that all of them showed good interaction with best docking scores dominated by hydrogen bonding with active site residues of α-helices 1 and 6. Both hydrophobic and hydrophilic amino acid residues of active site groove are paly a contributing role in the interaction with ligands. Auto Dock4.2 docking program used to performing molecular docking and it uses binding free energy evaluation to find the best binding mode. Fifty docked confirmations were obtained for each ligand and the confirmation with the highest docking energy values were selected as an optimal binding confirmation. The least and highest docking scores were found with the compounds SA36 and SA14 respectively, but both of them are not showing satisfactory ADMET

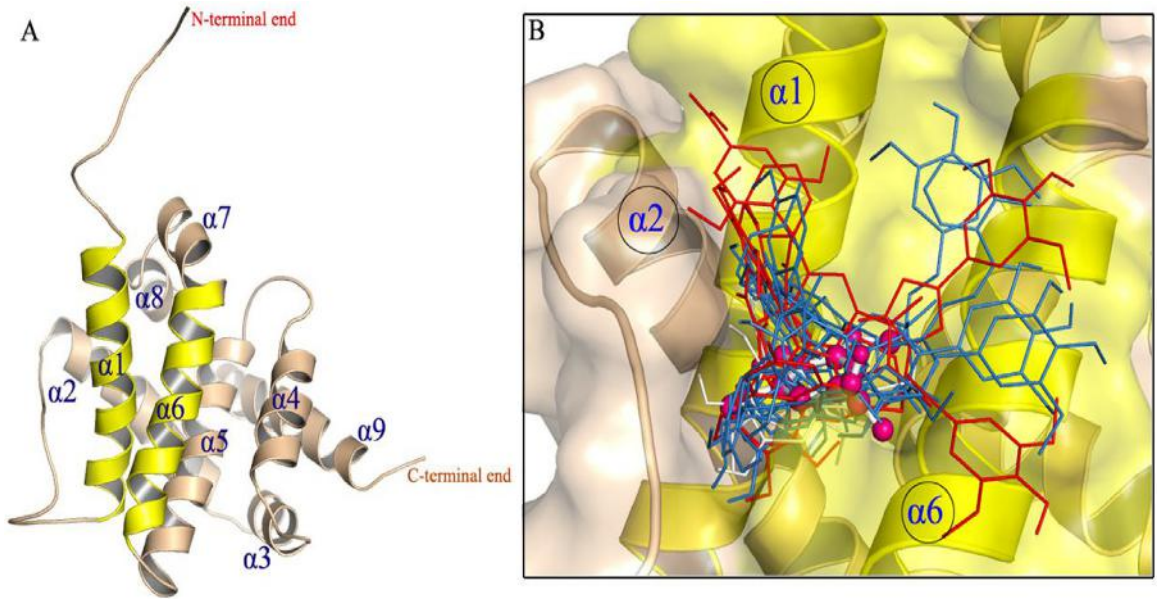

Fig. 1. A.Crystal structure of BAX and its BH3 trigger site (yellow helices). B. Binding mode of SA and its analogues at trigger site (yellow) of BAX. SA is shown in ball and stick model (pink) and its analogues represented in *lines*. (SA1, SA9, SA10, SA14 and SA21 are shown in red lines). (For interpretation of the references to colour in this figure legend, the reader is referred to the web version of this article.)

results with *in vitro* MDCK cell permeability. Among 29 compounds, SA, SA1, SA9, SA10, SA14 and SA21 with docking energy of −3.99, −5.73, −5.81, −5.79, −5.85 and −5.71 kcal/mol were selected for molecular interaction studies with BAX protein and the interaction modes of these docked compounds are depicted in Figs. 2 and 10(a, c & e). However, the reference compounds (BH3 mimetics) have shown docking energies in a range from negative to positive values viz., −6.67 (BAM-7), −4.85 (Obatoclax), −4.06 (Apogossypolone/ApoG2), −3.95 (MIM1), −2.75 (ABT-199), −2.25 (TW37), −2.20 (ABT-737), +2.91 (Apogossypol), +94.72 (Gossypol), +398.93 (BI-97C1/Sabutoclax), +889.14 (ABT-263/Navitoclax). BAM-7 has shown highest binding energy (-6.67 kcal/mol) with

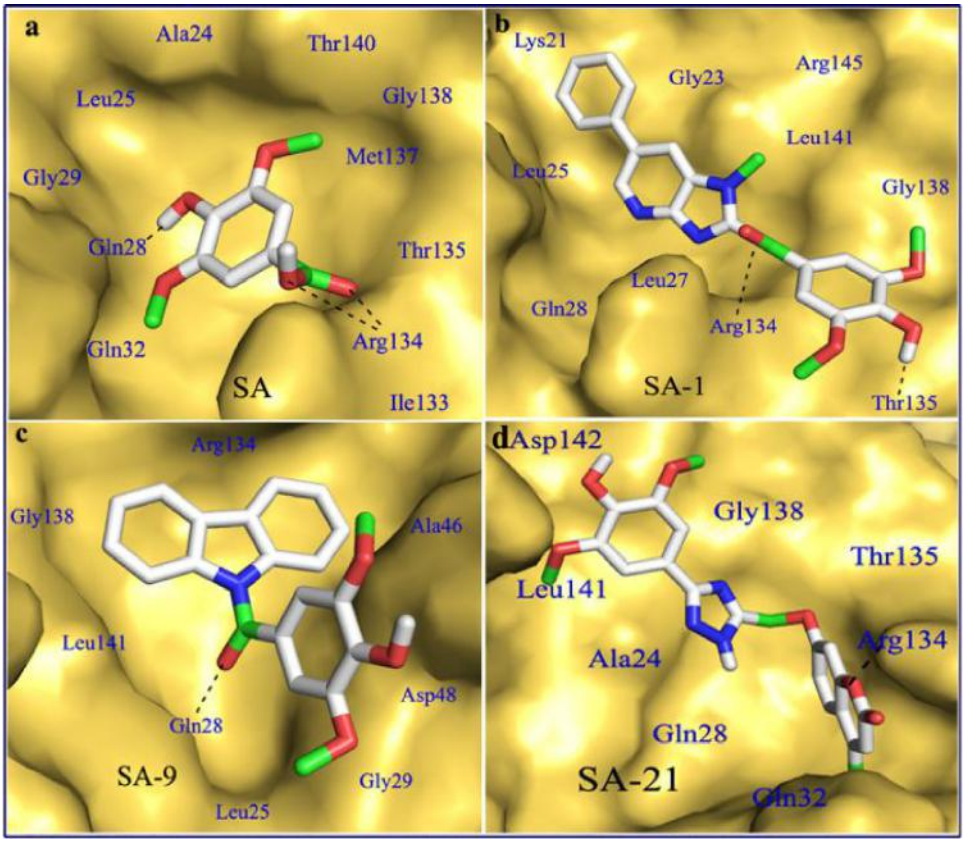

Fig. 2. The docked poses of SA, SA1, SA9, SA21 and its interactive residues within the BAX trigger site. Ligands are represented in stick forms and hydrogen bonds are shown in black dashed lines. (Docked images of BAM-7, SA-14 and SA-10 are illustrated in Fig.10).

BAX, which is found to be more than that of all SA analogues and other reference compounds examined in this study (Table 1). Molecular structures of docked SA analogues and reference compounds were shown in Figs. 3 and 4, respectively. Among all the SA docked analogues, SA14 showed highest docking score of −5.85 kcal/mol and which is higher than that of SA and its analogues and lower than that of BAM-7. SA9 and SA10 occupied the second and third ranks in the docking scores of all docked molecules. SA and SA8 have shown same docked energy of −3.99 kcal/mol. The BAX-ligand complexes have revealed that, the common residues involved in hydrogen bonding formation are Lys21, Gln28, Glu44, Ala46, Leu47, Asp53, Ser118, Ile133, Arg134, Thr135, Met137, Asp142, Glu146. The comparison of ligand binding residues and H-bond interaction of SA analogues and BH3 mimetics are summarized in Table 2. The distance between the H-bond interactions of all docked compounds were found in the range of 1.5–3.4 Å (<5 Å). In the hydrogen bonding, majority of donor atoms were from BAX residues and a very few were counted on SA analogues and reference compounds.

BAX activator molecule (BAM-7) was bound to the active site residues of Lys21, Gly29, Asp53, Met137, Leu141 and Leu161 depicted in Fig. 10 (a).The atoms of Asp (OD1&OD2) and Lys (HZ3) involved in hydrogen bonding interactions with the hydrogen (H11) and nitrogen atoms (N12&N18) of BAM-7 (Table 2). SA14 showed docking score of −5.85 kcal/mol with two hydrogen bonds with HZ2 of Lys21 and HG1 of Thr22 residues of BAX (Table 2), while parent compound SA (-3.99 kcal/mol) showed the lowest score among the selected compounds with establishment of three H-bonds between the H24, O7 and O8 atoms of SA and atoms of OE1 (Gln28), HH21 (Arg134) and HE (Arg134) respectively (Table 2). The addition of halogenated furan ring to the hydroxyl group of SA led to significantly influence the affinity and potency of among all designed compounds. The possible reason may be that insertion of halogen atoms in the led compounds was predominantly performed to steric effects, through the ability of these bulk atoms occupy the deeper pockets of target protein and it favors to contribute the stability of drug-target complex (Gillis et al., 2015). In the chemical point of view, insertion of halogens in the new chemical entities increases the lipophilicity, oral bioavailability and CNS penetration (Gerebtzoff et al., 2004; Gentry et al., 1999). SA14 was shown poor CNS penetration and significant good values for LogP and oral bioavailability. The proposed binding mode of SA14 in Fig. 10(c), suggested that, it was surrounded by the binding pocket of six residues of Gln18, Lys21, Thr22, Arg109, Phe114, Leu132 and Ile136. The oxygen atoms of the SA, SA1 and SA21 share common amino acid Arg134 for the formation of hydrogen bond. The OE1 atom of the Gln28 shown hydrogen bond interactions with the ligand atoms of SA (H24) and SA9 (O14) shown in Fig. 2a&c. SA10 has formed single hydrogen bond with HZ1 atom of Lys21 and also shown non-bonding interactions with Glu17, Leu25, Leu141, Arg145 and Leu149 of BAX residues, shown in Fig. 10(e). The results obtained from this docking study revealed that all the proposed docked ligands involved in the interaction of active site residues of BAX in direct mode or indirect mode. The obtained models demonstrate that, the atoms in the side chains that are added onto SA are mainly involved in the interaction with amino acid residues of BAX binding pocket. The oxygen atoms present on the ligands are essential for interaction with the residues of protein.

Apoptosis regulating signaling pathways and mitochondrial factors are often compromised to resistant during cell transformation, and it is an exciting challenge to develop small molecules or BH3 mimetics capable of inducing apoptosis in cancer cells. The BH3-only proteins are able to directly bind and activate BAX and Bak proteins are critical for cell death. Exploitation of the BH3-only protein features provides clues for the development of therapeutic anti-cancer drugs. For the past decade a number of BH3 mimetic drugs were produced. The BH3 mimetics are either peptides or synthetic molecules identified from random screening of natural products libraries or designed/improved by rational structure-based techniques. In the present study we designed a library of SA analogues through computational approaches and compared their binding interactions with BAX. Some clinically tested well known BH3 mimetics like BAM-7, Obatoclax, Apogossypolone/ApoG2, MIM1, ABT-199, TW37, ABT-737,Apogossypol, Gossypol, BI-97C1/Sabutoclax, ABT-263/Navitoclax were used as reference compounds in this comparative studies (Fig. 4 & S13 (A–K)). Docking analysis revealed that BAM-7 has shown best BH3 mimetic compared to other BH3 mimetics as well as SA analogues. In the overall study, SA analogues have shown more docking energy with BAX, compared to known BH3 mimetics.

Table 1
Comparison of docking energy of SA analogs and BH3 mimetics on BAX trigger site calculated by Auto Dock4.2.

Compound	[a]Total clusters	[b]Binding energy (kcal/mol)	Intermolecular energy (kcal/mol)	Torsional energy (kcal/mol)	Internal energy (kcal/mol)	Inhibition constant (μM)	[c]RMS deviation (Å)
SA	27	−3.99	−4.77	1.37	−0.59	1180	0.24
SA1	12	−5.73	−6.62	1.65	−0.75	63.15	0.91
SA9	15	−5.81	−6.09	1.10	−0.82	55.01	0.72
SA10	13	−5.79	−6.15	1.10	−0.75	56.66	1.44
SA14	2	−5.85	−7.03	1.92	−0.74	51.38	0.56
SA21	1	−5.71	−6.50	1.92	−1.13	65.08	1.42
BAM-7	7	−6.67	−5.95	1.65	−2.37	12.83	0.36
Obatoclax	5	−4.85	−6.04	1.19	−1.47	279.73	1.62
Apogossypolone/ ApoG2	20	−4.06	−6.14	2.09	1.29	1060	1.26
MIM1	8	−3.95	−5.74	1.79	−2.71	1280	1.00
ABT-199	1	−2.75	−6.63	3.88	−3.91	9570	0.82
TW37	2	−2.25	−5.53	3.28	24.88	22510	0.93
ABT-737	3	−2.20	−6.98	4.77	−0.04	24280	1.90
Apogossypol	12	+2.91	1.46	2.47	−1.02	–	0.00
Gossypol	26	+94.72	91.44	3.28	−3.21	–	0.00
BI-97C1/ Sabutoclax	3	+398.93	394.46	4.47	102.1	–	0.00
ABT-263/ Navitoclax	2	+889.14	871.55	4.66	12.92	–	0.00

[a] The best clusters of a total 100 runs are shown.
[b] Value for the optimal structure in the cluster.
[c] The geometry fit was measured by r.m.s. deviation of angles.

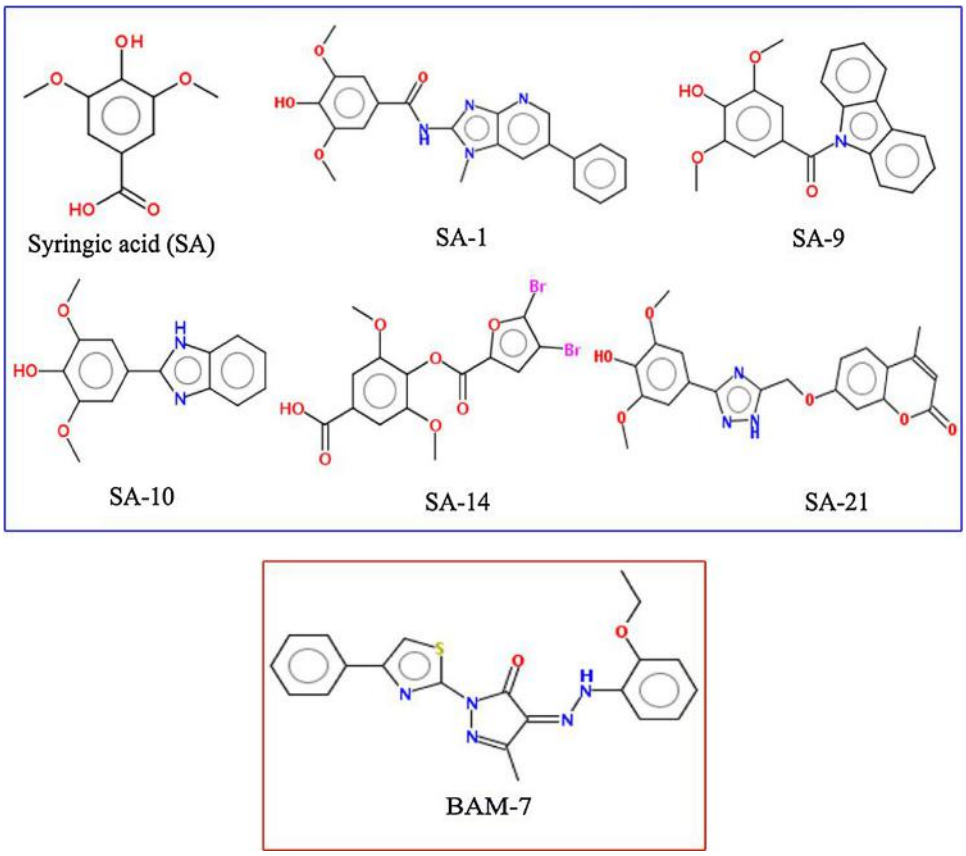

Fig. 3. Structures of best docking hits of SA analogues and BAM-7(the direct BAX activator molecule) examined in this study.

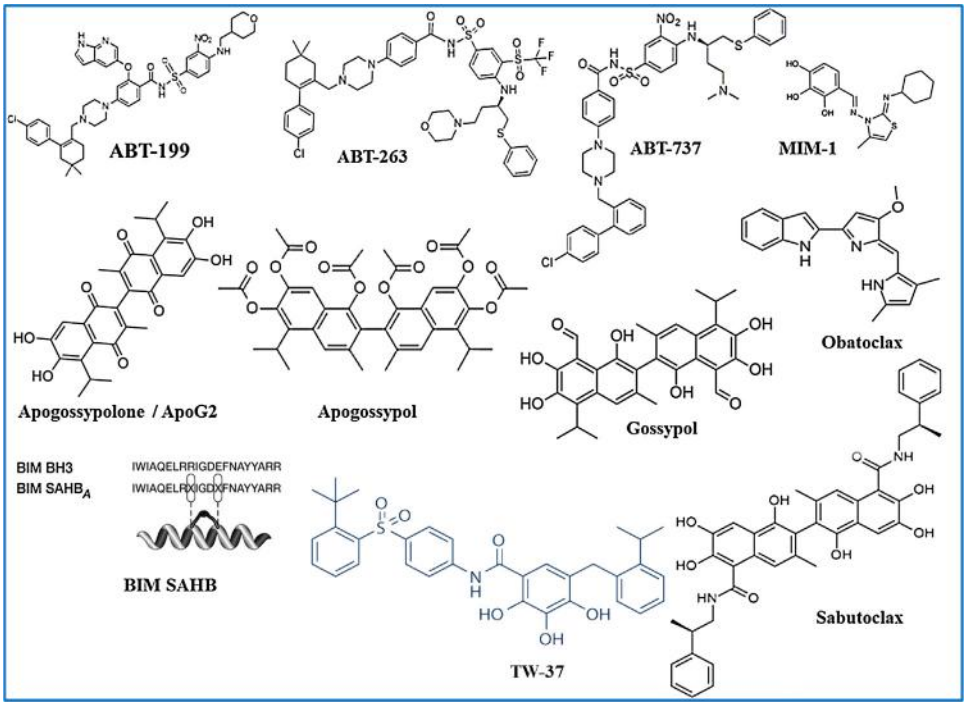

Fig. 4. Chemical structures of clinically tested BH3 mimetics.

The prototype BH3 mimetic ABT-737 selectively targets the three prosurvival proteins BCL-XL, BCL-2, and BCL-W and its oral derivative ABT-263 (navitoclax) can induce BAX/BAK-dependent apoptosis *in vitro* and have antitumor effects in animal models (Tse et al., 2008; Van Delft et al., 2006). At molecular level, docking analysis of these two molecules (ABT-737 and ABT-263) suggested that, binds with Lys21 of the BAX trigger site and it may accountable for BAX induction (Fig. S13-C&B). The derivative of

Table 2
Comparison of ligand binding residues and H-bonding interaction of SA analogs and BH3 mimetics at BAX trigger site.

Compound	H-bond interaction		Distance (Å)	Donor atom	Acceptor atom
	Protein	Ligand			
	Gln28:OE1	H	2.0	OE1	H
SA	Arg134:HH21	O	1.8	HH21	O
	Arg134: HE	O	1.9	HE	O
	Thr135:OG1	H	2.2	OG1	H
SA1	Arg134: CO	H	2.2	CO	H
SA9	Gln28: OE1	O	3.5	OE1	O
SA10	Lys21: HZ1	O	2.0	HZ1	O
SA14	Lys21: HZ2	O	1.6	HZ2	O
	Thr22:HG1	O	2.0	HG1	O
SA21	Arg134: HH21	O	2.2	HH21	O
BAM-7	Asp53: OD1	H	2.0	OD1	H
	Asp53: OD2	N	3.4	OD2	N
	Lys21: HZ3	N	1.9	HZ3	N
Obatoclax	Leu47: CO	N	3.2	CO	N
	Leu47: CO	H	1.9	CO	H
Apogossypolone/ ApoG2	Arg145:HH11	O	1.8	HH11	O
MIM1	Met20:CO	H	2.3	CO	H
	Lys21:HZ1	O	2.4	HZ1	O
	Lys21:CO	H	2.4	CO	H
ABT-199	Lys21:HZ3	O	1.8	HZ3	O
	Asp53:OD2	O	3.4	OD2	O
TW37	Lys21:HZ1	O	2.5	HZ1	O
	Lys21:HZ1	O	2.3	HZ1	O
ABT-737	–	–	–	–	–
Apogossypol	Lys21:CO	H	2.3	CO	H
Gossypol	Met137:CO	O	2.6	CO	O
	Ile133:CO	H	2.1	CO	H
BI-97C1/ Sabutoclax	Thr140:CO	H	2.5	CO	H
	Ser118:NH	H	2.9	NH	H
	Phe30:CO	H	2.6	CO	H
ABT-263/ Navitoclax	Lys21:HZ2	O	1.5	HZ2	O
	Met20:CO	O	3.4	CO	O
BIM-SAHB (peptide)	Lys21:HZ1	Ala164:CO	1.8	HZ1	Ala164:CO
	Lys21:HZ3	Ala161:CO	2.6	HZ3	Ala161:CO
	Glu17:OE2	Ala164:CN	2.7	OE2	Ala164:CN
	Glu146:OE2	Arg153:NH1	3.3	OE2	Arg153:NH1
	Asp142:OD2	Arg153:NE	3.4	OD2	Arg153:NE

cycloprodigiosin, GM15-070 (Obatoclax) can activated apoptosis via releasing Bak from Mcl-1 and Bim from Bcl-2 and Mcl-1 (Konopleva et al., 2008). The *in silico* hypothesis of Obatoclax shown that, interaction of Leu47 of the BAX trigger site may release the BAX from its counterpart, Bcl2 (Fig. S13-H). The other BH3 mimetics Gossypol and its derivatives such as apogossypol and apogossypolone (ApoG2) are currently in preclinical evaluation, whereas the benzoylsulfonide derivative TW37 has already reached phase I/II trials (Arnold et al., 2008; Lessene et al., 2008; Azmi et al., 2011; Quinn et al., 2011a, 2011b; Wei et al., 2011). All these compounds have similar binding capacities with moderate affinity and induce BAX mediated apoptosis in various cancer cells. The molecular interactions of these compounds with BAX has revealed that, binding at α-helices 1 and 6 of BAX trigger site may induce the conformational change of BAX, which leads to mitochondrial mediated cell death (Fig. S13-D,E,F&J). Gavathiotis and colleagues have reported that SAHB derived from the BIM BH3 helix can directly bind to BAX at an interaction site (Gavathiotis et al., 2008). The docking study of BIM SAHB (PDB: 2YQ6) with BAX was shown that, SAHB binds at hydrophobic BAX trigger site and form hydrogen bond interactions with Lys21, Glu17, Glu146 and Asp142 residues (Fig. S13-K). The SA analogues have shown similar kind of interactions with BAX like other BH3 mimetics examined in the present study. By the above information we can strongly hypothesized that designed SA analogues may induce the BAX mediated apoptosis in cancer cells. Along with these BH3 mimetics, recently identified several molecules which induced the apoptosis through BAX activation. A data on Morusin (isolated from the root bark of *Morus alba* L.) has been demonstrated to modulate the expression of the anti-apoptotic protein Survivin and pro-apoptotic protein BAX in human breast cancer cells (Kang et al., 2017). The Myricetin, a flavonoid reported to induce apoptotic cell death in HepG2 human hepatocarcinoma cells and HCT-15 human colon cancer cells *via* increasing the BAX/BCL2 (Kim et al., 2014). The BAX Targeting Compound (BTC-8), a derivative of BAM-7 alone or in combination with the alkylating agent TMZ, was evaluated in human Glioblastoma cells and it was demonstrated to

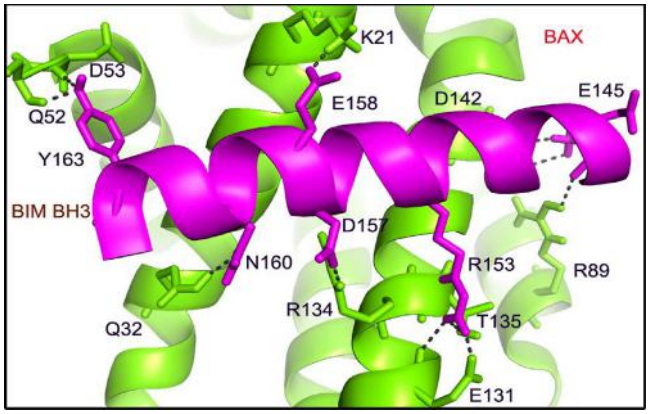

Fig. 5. The proposed model of BAX/BIM BH3 interaction (BAX and BIM BH3 is represented in Green Limon and Magentas helices respectively). The picture depicted the H-bond interactions between BAX and BimBH3 residues at BAX trigger site. (For interpretation of the references to colour in this figure legend, the reader is referred to the web version of this article.)

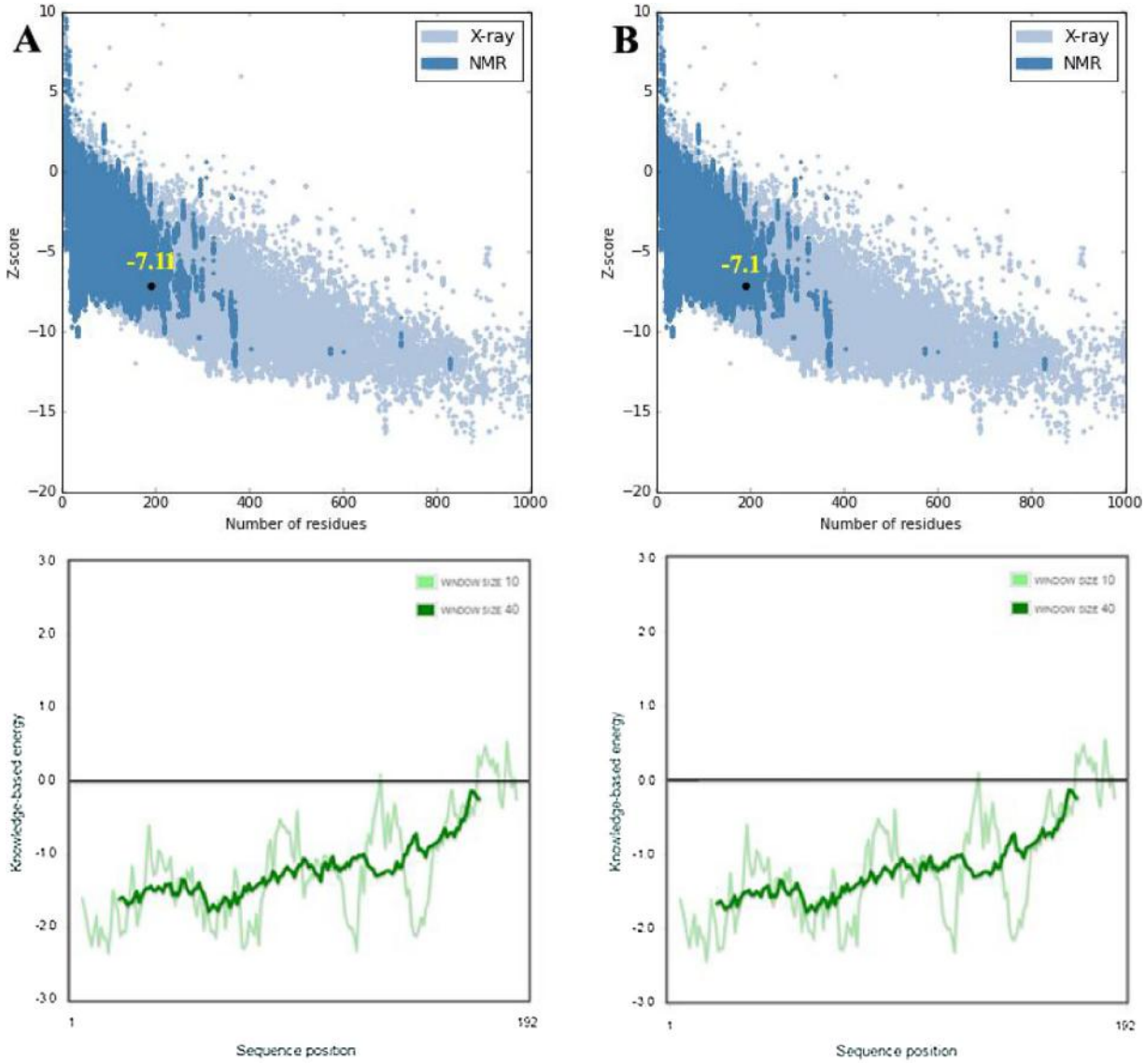

Fig. 6. Z-score (overall model quality) and energy plots (local model quality) for the (A) wild type; (B) K21E mutant generated through ProSA web server. The area of light blue and dark blue indicates the Z-scores of protein chains (PDB) developed by X-ray crystallography and NMR spectroscopy respectively. Black dot represents the Z-score value of protein model. (For interpretation of the references to colour in this figure legend, the reader is referred to the web version of this article.)

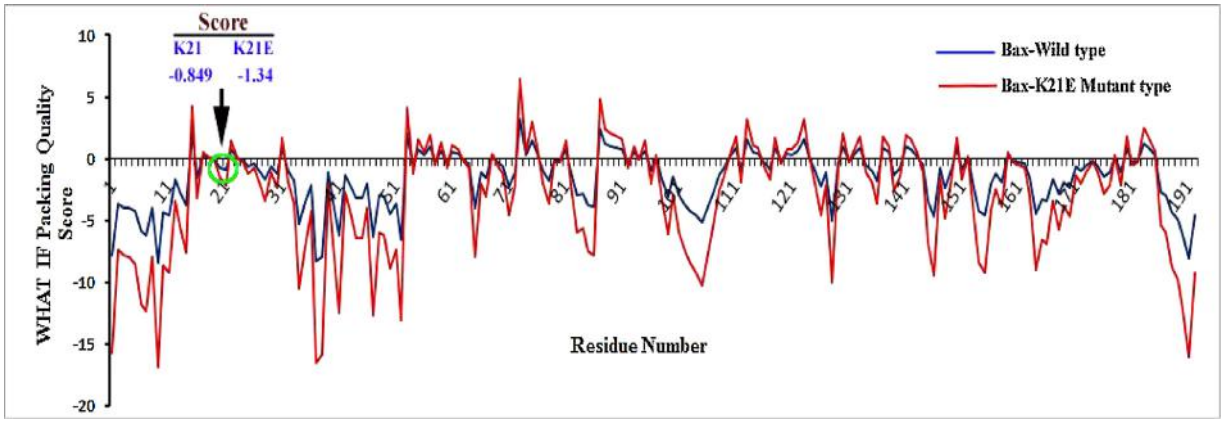

Fig. 7. Comparative WHAT IF packing quality control (PQC) scores of wild type and mutant types of BAX.

inhibit Glioblastoma cell proliferation through the induction of mitochondrial membrane permeabilization (Daniele et al., 2018). The effect of doxorubicin induces mitochondrial-dependent apoptosis by down-regulation of Bcl-xL and up- regulation of BAX and caspase-9 expression in Breast Cancer Cells (Sharifi et al., 2015). A recent data has suggested that an active compound Cinobufagin (CBF) isolated from secretory glands of *Bufo gargarizans* can significantly increase BAX expression and decrease Bcl-2 expression in MCF-7 cells (Zhu et al., 2018).

The BAX activation requires the interaction of Lys21 with the Glu158 of BAX activator molecule, BIM BH3 helix. K21E mutation of BAX leads to decrease in strength of interaction with its activator. Among all SA analogues examined in the present study, SA-10 and SA-14 only can interact with K21 of BAX and showed good docking energies compared with other BH3 mimetics. For the clear evidence of K21 interaction with activator molecules, we have performed mutation analysis for comparative study of docking mode, binding strength, ligand flexibility for wild type

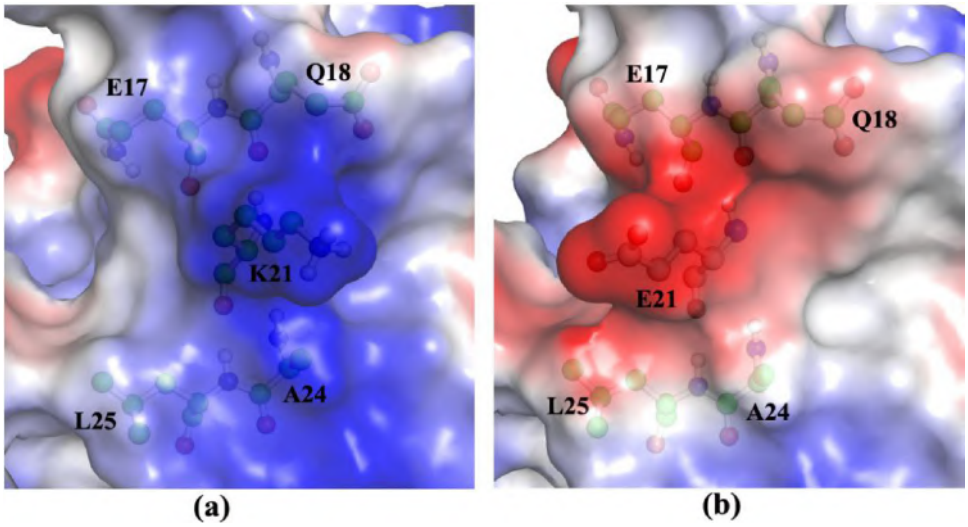

Fig. 8. Surface diagram of wild type and mutant type (K21E) of BAX. The surface potentials are different in wild type (a) and mutant type (b), and colors on surface are based on electrostatic potential and bound residues (ball and stick) in protein. The potential energy of wild type and mutant type is $-45.607k_bT/e$ to $+45.607k_bT/e$; $-59.297\ k_bT/e$ to $+59.297k_bT/e$ respectively, where k_b, T, and e are the Boltzmann constant, temperature and the electron charge, respectively).

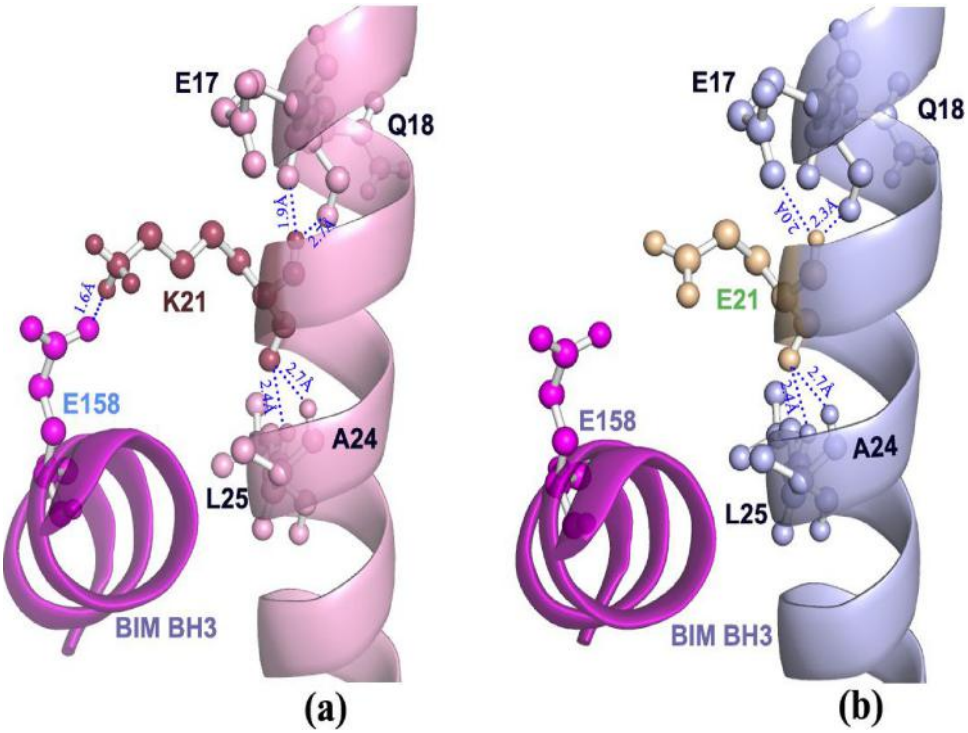

Fig. 9. Inter and intra molecular contacts in BIM BH3/BAX complex of WT and K21E. Model structure of wild type (a) and K21E mutant type (b) of BAX with BIM BH3 peptide is shown in helices. Interacting residues are shown in ball and stick model and hydrogen bond interactions are represented as blue dotted lines. K21E point mutation reduces the hydrogen bond interaction with E158 of BIM BH3 (b) and impaired the helix structure by altering the H-bond distances (Å) of E17 and Q18 in wild and mutant types. (For interpretation of the references to colour in this figure legend, the reader is referred to the web version of this article.)

and mutant type of protein. For these, SA-10, SA-14 and BAM-7 have been taken as ligands against mutant type of protein for docking studies.

3.4. BAX_{K21E} mutation

The point mutation of BAX occurs in helix1 but does not disturb the overall conformation of α-helical secondary structure. The change at residue 21 from Lys to Glu point mutation was generated using *in silico* mutagenesis pyMOL wizard. Glu158 of BIM BH3 peptide forms intermolecular hydrogen bond with the side chain of Lys21 of BAX (Fig. 5). However, the Lys and Glu residues are differ in charge and size. Substitution of lysine to glutamic acid results in a minute changes in ProSA-web Z-score, from−7.11 to−7.1 (Fig. 6), while there was no change in Verify 3D score (0.53) (Fig not shown). The compatibility between sequence and its structure can be calculated using energy function ProSA-web Z-score. The minor fluctuation observed in Z-score value of mutant protein is −7.1; it shows that changes came about local model quality of protein by substitution of amino acid residue. The Lys21Glu point mutation in BAX produces a minor local conformational change by observing the intra and intermolecular hydrogen bonding interactions with contiguous residues. WHAT IF is also used to check the normality of the local environment of amino acids. The WHAT IF evaluation shown that, point mutation leads to change in local environment of amino acid residues in protein model (Fig. 7). The electrostatic potential energy for the native and mutant protein is $-45.607k_bT/e$ to $+45.607k_bT/e$ and $-59.297k_bT/e$ to $+59.297k_bT/e$ respectively (where k_b, T, and e are the Boltzmann constant, temperature and the electron charge, respectively). The surface potentials for wild and mutant protein

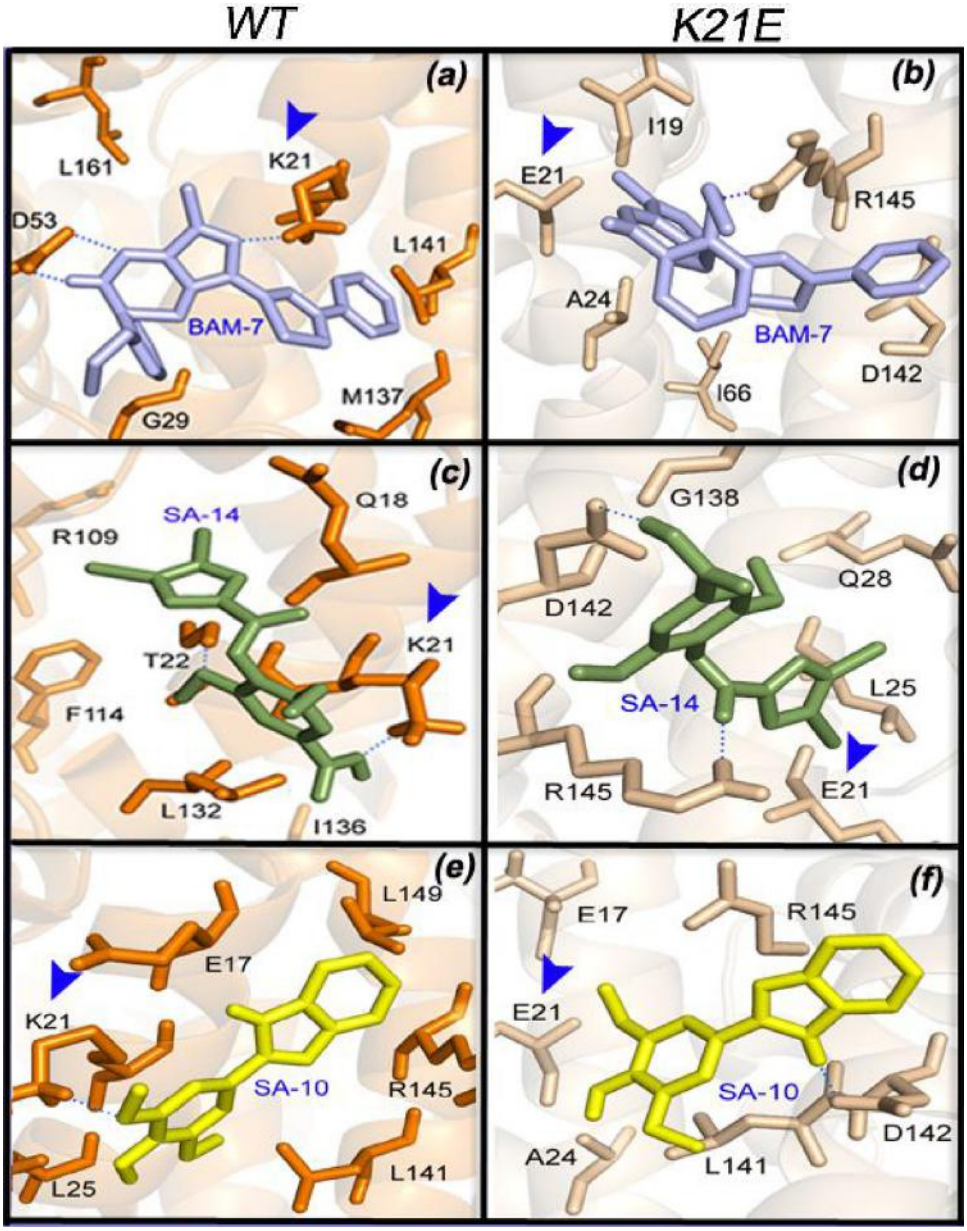

Fig. 10. Binding interactions of BAM-7, SA-14 and SA-10 with the selectivity filter in WT (a, c & e) and K21E mutant (b, d &f) of BAX. The blue arrow heads represent the wild (K21) and mutant (E21) residues. The hydrogen bonds are shown in blue lines. The image illustrated the position and orientation of ligands and changed interactive residues at trigger site of wild and mutant type of BAX. (For interpretation of the references to colour in this figure legend, the reader is referred to the web version of this article.)

are shown in Fig. 8. The changes in potential energy are supported for the stability of protein structure. Structural changes of protein determined by its amino acid composition and any mutation occurs at specific position creates difference in potential energy. It is conformed that the substitution of any residue modifies energy and stability of protein. Hydrogen bonding interaction (inter & intra) was observed in native and mutant protein is reduced, depicted in Fig. 9. In native structure of BAX, lys21 forms hydrogen bond (1.6 Å) with side chain of Glu158 of BIM BH3 peptide (Fig. 9a) however; the mutation creates reduction of this hydrogen bond (Fig. 9b). The length of hydrogen bond distances was observed at local residues interacts with lysine or glutamic acid of native and mutant proteins. E17, Q18, A24 and L25 residues forms intra molecular hydrogen bonds with lysine or glutamic acid and confers its protein stability. The change in hydrogen bond length determines the local conformation of helices and its stability. Here, E17 and Q18 residues hydrogen bonded with K21 or E21, the changes observed that bond length is differ in wild and mutant type of protein. The changed hydrogen bond length of E17 is 1.9 Å to 2.0 Å; Q18 is 2.7 Å to 2.3 Å for wild type and mutant type respectively (Fig. 9a&b). The minor change in local structure determines total structural stability of protein.

Table 3
Difference in docking energy of binding and inhibition constant calculated by AutoDock4.2 for WT and K21E.

Compound	Docking energy (kcal/mol)			Inhibition constant (μM)		
	WT	K21E	Difference WT vs K21E	WT	K21E	Difference WT vs K21E
BAM-7	−6.67	−5.68	−0.99	12.83	69.13	56.3
SA-14	−5.85	−4.33	−1.52	51.38	674.92	623.54
SA-10	−5.79	−4.15	−1.64	56.66	911.6	854.5

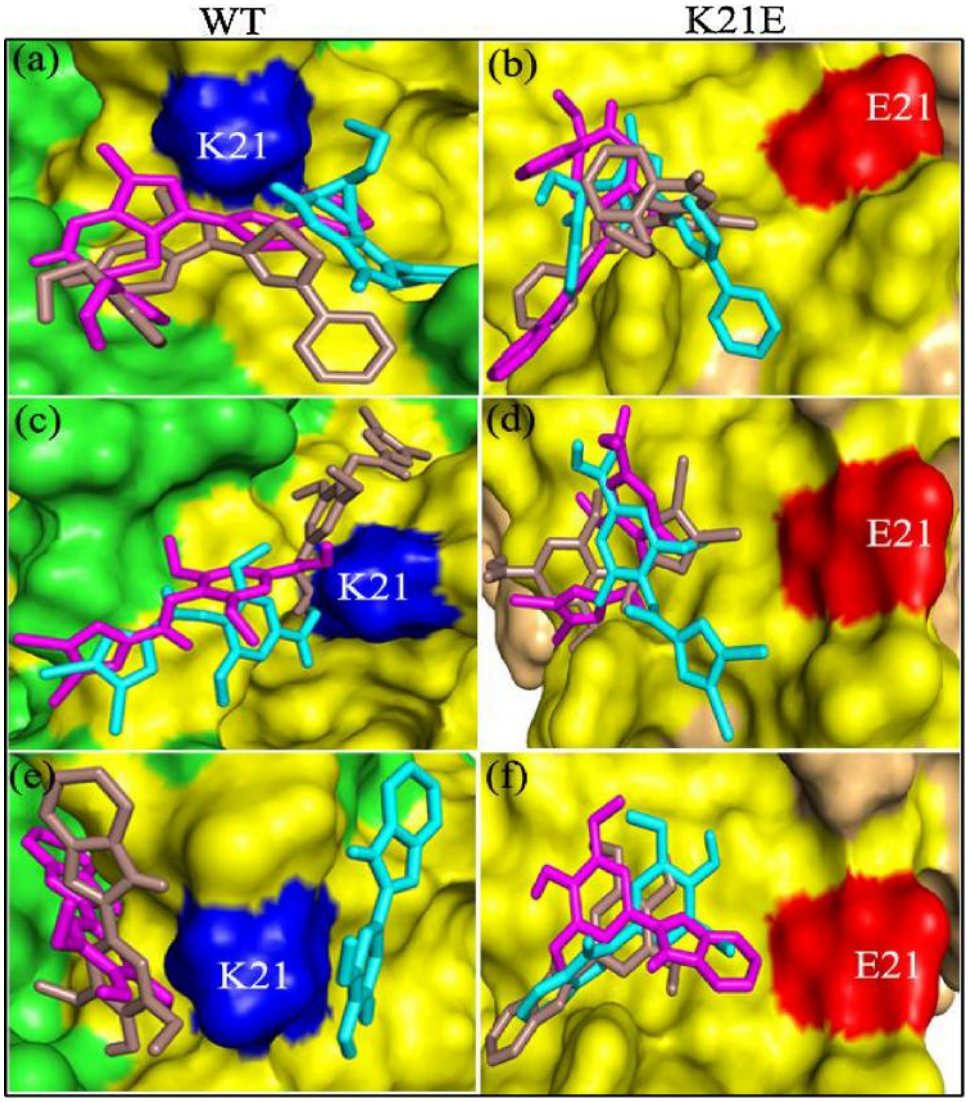

Fig. 11. Docked ligand conformations at trigger site of WT and BAX $_{K21E}$. The docking energy of first three ranked ligands (BAM-7(a, b); SA-14(c, d) and SA-10 (e, f)) demonstrates the binding mode and flexibility at the trigger site of wild and mutant type of BAX. The docking poses of ligands are more vicinity to K21 in WT than E21 in mutant type. The nearest conformers shown more docking energy in WT compared to mutant.

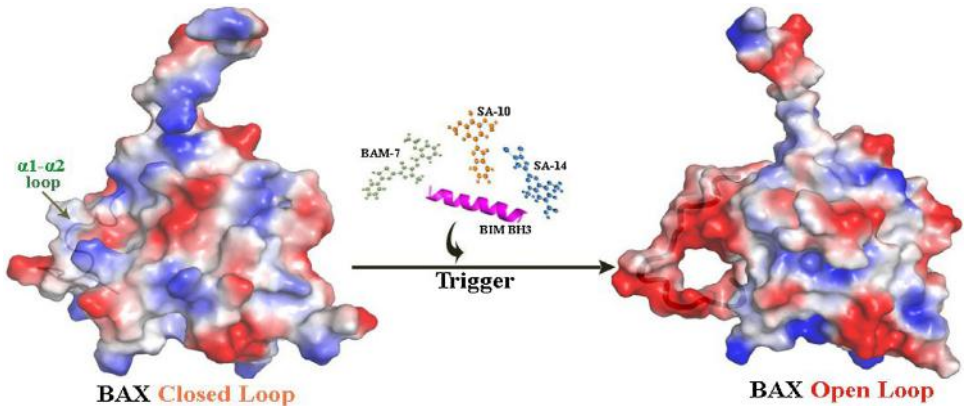

Fig. 12. *In Silico* predicted model of BAX activation is initiated by displacement of α1-α2 loop from closed to an open conformation induced by the ligands examined in the present study.

3.5. Assessment of wild type vs. mutant BAX$_{K21E}$differences via protein docking with ligands of SA-10, SA14 and BAM-7

The docking results revels that, point mutation of BAX at α1brings to change the binding energy, docking mode and flexibility of SA analogues and BAM-7 at trigger site. The mutation analysis can justify the stronger and weaker interactions of bound ligands at active sites of proteins. The lys21 is the crucial step for the activation of BAX upon interaction with ligand molecules. Fig. 10 depicts the observation of difference in ligand flexibility at the Lys21 site of BAX. Mutation directs the docking mode of ligands from native to unusual form by changing the binding interaction of amino acids. BAM-7 hydrogen bonded with R145 of mutant type and shown hydrophobic interactions with E21, A24, I19, I66 and D142; however the same ligand which forms three hydrogen bonds with wild type residues of BAX. The docking energy of mutant with BAM-7 reduced to −5.68 kcal/mol from the wild type value of −6.67 kcal/mol. The similar criteria i.e. reduced docking energy and binding constants were happened for SA analogues (SA-10 and SA-14). The difference in docking score and inhibition constant for the wild and mutant type was summarized in Table 3. Three ligands examined in the docking study on mutant type have different functional groups in their chemical moiety. The docking energy of mutant was found to be lower than that of wild type of protein, stating that the mutant model (BAX_{K21E}) had a weaker binding affinity for ligands. Hydrogen bond confers the great stability of protein-ligand complexes; a large number of hydrogen bonds form more stable complexes (Steiner and Koellner, 2001). The docking study of protein-ligand binding mechanism of native and mutant reveals that mutant has weaker interaction with ligands than its native type of protein model. Ensemble docking was applied to the rigid protein structure for the reasonable conformations and proper hydrogen bond formation of ligands at its active site. A single docking conformation of ligand can failed to explain the correct binding mode and hydrogen bond interactions with receptor. In the present study, we organized the docked ligands (BAM-7, SA-10 & SA-14) based on their lowest binding energy hierarchy. The compounds with highest docking energy are occupied very close to the Lys21 of native type, where as in mutant type occupied away from the Glu21 residue. The nearest conformers to the k21/E21 residue were shown in dark salmon (red) color, represented in Fig. 11. The actual binding and interaction requires the fitting of ligands at binding pockets propinquity to target residue (K21), it is successful with the first ranked position of bound ligands (dark salmon color sticks). Initiation of BAX activation occurs trough the expose of amino acid residues from 12 to 24, which is taken away by α1-α2 loop displacement. BIM SAHB and BAM-7 directly engages the BAX trigger site by producing steric hindrance at the junction of α1-α2 loop. *In silico* predicted model of BAX activation through displacement of α1-α2 loop from closed to an open conformation induced by the ligands represented in Fig. 12. Flexibility and conformation of ligands determined by its specific functional groups, such as methylated compounds express more energy than its counter parts. The difference in docking energy, internal energy and inhibition constants were observed more in mutant than wild type of protein complex.

4. Conclusion

Among all virtually proposed SA analogues, only five; SA1, SA9, SA10, SA14 and SA21 showed highest docking energy with BAX protein, of which SA10 and SA14 specifically interact with Lys21 residue. From the docking results, we compared that SA analogues have shown best docking energies and detailed molecular interactions with BAX residues than BH3 mimetics. The results of *in silico* mutation of BAX from Lys21 to Glu21 decreased structural stability and reduced hydrogen bonding interactions with its BIM BH3 peptide. Comparative docking studies of SA10 and SA14 with wild and mutant types revealed differences in docking energy, inhibition constant and binding residues involved in hydrogen bond formation; BAM-7 also showed similar results with both types. By observing interaction of SA analogues (SA10 and SA14) and BAM-7 with wild and mutant proteins, we concluded that SA analogues showed almost similar activity with BH3 mimetic, BAM-7. The combined molecular modeling and mutation studies provide selection of small molecules as better interactive agents for the target proteins in cancer prevention.

Conflicts of interest

No competing interests exist.

Acknowledgments

The authors are grateful to, Indian Council of Medical Research (ICMR), Govt. of India, New Delhi for financial assistance to C. Srinivasulu and Department of Biotechnology-Bioinformatics infrastructure facility (DBT-BIF), Govt. of India, Department of Biochemistry, Sri Krishnadevaraya University, Anantapuramu, A.P, India for providing lab facilities for the research work. The research work was supported by Indian Council of Medical Research (ICMR) and Department of Biotechnology-Bioinformatics infrastructure facility (DBT-BIF), India.

Appendix A. Supplementary data

Supplementary data associated with this article can be found, in the online version, at https://doi.org/10.1016/j.compbiolchem.2018.03.003.

References

Abaza, M.S., Al-Attiyah, R., Bhardwaj, R., Abbadi, G., Koyippally, M., Afzal, M., 2013. Syringic acid from Tamarixaucheriana possesses antimitogenic and chemo-sensitizing activities in human colorectal cancer cells. Pharm. Biol. 51, 1110–1124.

Arnold, A.A., Aboukamel, A., Chen, J., Yang, D., Wang, S., Al-Katib, A., et al., 2008. Preclinical studies of apogossypolone: a new nonpeptidic pan smallmolecule inhibitor of Bcl-2, Bcl-XL and Mcl-1 proteins in follicular small cleaved cell lymphoma model. Mol. Cancer 7, 20.

Azmi, A.A., Wang, Z., Philip, P.A., Mohammad, R.M., Sarkar, F.H., 2011. Emerging Bcl-2 inhibitors for the treatment of cancer. Expert Opin. Emerging Drugs 16, 59–70.

Baell, J.B., Huang, D.C.S., 2002. Prospects for targeting the Bcl-2 family of proteins to develop novel cytotoxic drugs. Biochem. Pharmacol. 64, 851–863.

Belkheiri, N., Bouguerne, B., Bedos-Belval, F., Duran, H., Bernis, C., Salvayre, R., Nègre-Salvayre, A., Baltas, M., 2010. Synthesis and antioxidant activity evaluation of a syringic hydrazones family. Eur. J. Med. Chem. 45 (7), 3019–3026.

Berman, H.M., Battistuz, T., Bhat, T.N., Bluhm, W.F., Bourne, P.E., Burkhardt, K., Feng, Z., Gilliland, G.L., Iype, L., Jain, S., Fagan, P., Marvin, J., Padilla, D., Ravichandran, V., Schneider, B., Thanki, N., Weissig, H., Westbrook, J.D., Zardecki, C., 2002. The protein data bank. Acta Crystallogr. D: Biol. Crystallogr. 58, 899–907.

Bowie, J.U., Luthy, R., Eisenberg, D., 1991. A method to identify protein sequences that fold into a known three-dimensional structure. Science 253, 164–170.

Cheemanapalli, S., Anuradha, C.M., Madhusudhana, P., Mahesh, M., Raghavendra, P. B., Kumar, C.S., 2016. Exploring the binding affinity of novel syringic acid analogues and critical determinants of selectivity as potent proteasome inhibitors. Anticancer Agents Med Chemistry 16, 1496–1510.

Daniele, S., Pietrobono, D., Costa, B., Giustiniano, M., La Pietra, V., Giacomelli, C., La Regina, G., Silvestri, R., Taliani, S., Trincavelli, M.L., Da Settimo, F., Novellino, E., Martini, C., Marinelli, L., 2018. Bax activation blocks self-renewal and induces apoptosis of human glioblastoma stem cells. ACS Chem. Neurosci. 9, 85–99.

Delano, W.L., 2006. The PyMOL Molecular Graphics System. Delano Scientific, SanCarlos, CA, USA. http://www.pymol.org.

Delgado-Soler, L., Pinto, M., Tanaka-Gil, K., Rubio-Martinez, J., 2012. Molecular determinants of Bim (BH3) peptide binding to pro-survival proteins. J. Chem. Inf. Model 52, 2107–2118.

Gavathiotis, E., Suzuki, M., Davis, M.L., Pitter, K., Bird, G.H., Katz, S.G., Tu, H.C., Kim, H., Cheng, E.H., Tjandra, N., Walensky, L.D., 2008. BAX activation is initiated at a novel interaction site. Nature 455 (7216), 1076–1081.

Gavathiotis, E., Reyna, D.E., Davis, M.L., Bird, G.H., Walensky, L.D., 2010. BH3-triggered structural reorganization drives the activation of proapoptotic BAX. *Mol.* Cell 40, 481–492.

Gavathiotis, E., Reyna, D.E., Bellairs, J.A., Leshchiner, E.S., Walensky, L.D., 2012. Direct and selective small-molecule activation of proapoptoticBaX. Nat. Chem. Biol. 8 (7), 639–645.

Gentry, C.L., Egleton, R.D., Gillespie, T., Abbruscato, T.J., Bechowski, H.B., Hruby, V.J., Davis, T.P., 1999. The effect of halogenation on blood-brain barrier permeability of a novel peptide drug. Peptides 20 (10), 1229–1238.

Gerebtzoff, G., Li-Blatter, X., Fischer, H., Frentzel, A., Seelig, A., 2004. Halogenation of drugs enhances membrane binding and permeation. Chembiochem 5 (5), 676–684.

Gillis, E.P., Eastman, K.J., Hill, M.D., Donnelly, D.J., Meanwell, N.A., 2015. Applications of fluorine in medicinal chemistry. J. Med. Chem. 58 (21), 8315–8359.

Irvine, J.D., Takahashi, L., Lockhart, K., Cheong, J., Tolan, J.W., Selick, H.E., Grove, J.R., 1999. MDCK (Madin-Darby canine kidney) cells: a tool for membrane permeability screening. J. Pharm. Sci. 88, 28–33.

Kang, S., Kim, E.O., Kim, S.H., Lee, J.H., Ahn, K.S., Yun, M., Lee, S.G., 2017. Morusin induces apoptosis by regulating expression of Bax and Survivin in human breast cancer cells. Oncol. Lett. 13, 4558–4562.

Karthik, Gowri, Angappan, Mangalagowri, Vijaya Kumar, Arun kumar, Natarajapillai, Sukumaran, 2014. Syringic acid exerts antiangiogenic activity by downregulation of VEGF in zebrafish embryos. Biomed. Prevent. Nutr. 4, 203–208.

Kazi, A., Sun, J., Doi, K., Sung, S.S., Takahashi, Y., Yin, H., Rodriguez, M.J., Becerril, J., Berndt, N., Hamilton, D.A., Wang, G.H., Sebti, M.S., 2011. The BH3 a-helical mimic BH3-M6 disrupts Bcl-XL, Bcl-2, Bad, or Bim and induces apoptosis in a Bax- and Bim-dependent manner. J. Biol. Chem. 286, 9382–9392.

Kim, M.E., Ha, T.K., Yoon, J.H., Lee, J.S., 2014. Myricetin induces cell death of human colon cancer cells via BAX/BCL2-dependent pathway. Anticancer Res. 34, 701–706.

Konopleva, M., Watt, J., Contractor, R., Tsao, T., Harris, D., Estrov, Z., Bornmann, W., Kantarjian, H., Viallet, J., Samudio, I., Andreeff, M., 2008. Mechanisms of antileukemic activity of the novel Bcl-2 homology domain-3 mimetic GX15-070 (obatoclax). Cancer Res. 68, 3413–3420.

LaBelle, J.L., Katz, S.G., Bird, G.H., Gavathiotis, E., Stewart, M.L., Lawrence, C., Fisher, J. K., Godes, M., Pitter, K., Kung, A.L., Walensky, L.D., 2012. A stapled Bim peptide overcomes apoptotic resistance in hematologic cancers. J. Clin. Invest. 122, 2018–2031.

Lessene, G., Czabotar, P.E., Colman, P.M., 2008. Bcl-2 family antagonists for cancer therapy. Nat. Rev. 7, 989–1000.

Lipinski, C.A., Lombardo, F., Dominy, B.W., Feeney, P.J., 1997. Experimental and computational approaches to estimate solubility and permeability in drug discovery and development settings. Adv. Drug Deliv. Rev. 23, 3–25.

Lipinski, C.A., Lombardo, F., Dominy, W., Feeney, P.J., 2001. Experimental and computational approaches to estimate solubility and permeability in drug discovery and development settings. Adv. Drug Del. Rev. 46, 3–26.

Luthy, R., Bowie, J.U., Eisenberg, D., 1992. Assessment of protein models with three-dimensional profiles. Nature 356, 83–85.

Morris, G.M., Huey, R., Lindstrom, W., Sanner, M.F., Belew, R.K., Goodsell, D.S., Olson, A.J., 2009. AutoDock4 and AutoDockTools4: Automated docking with selective receptor flexibility. J. Comput. Chem. 30, 2785–2791.

Nguyen, M., Marcellus, R.C., Roulston, A., Watson, M., Serfass, L., Murthy Madiraju, S. R., Goulet, D., Viallet, J., Belec, L., Billot, X., Acoca, S., Purisima, E., Wiegmans, A., Cluse, L., Johnstone, R.W., Beauparlant, P., Shore, G.C., 2007. Small molecule obatoclax (GX15-070) antagonizes MCL-1 and overcomesMCL-1-mediated resistance to apoptosis. Proc. Natl. Acad. Sci. U. S. A. 104, 19512–19517.

Nuessler, V., Stotzer, O., Gullis, E., Pelka-fleischer, R., Pogrebnaik, A., Gieseler, F., Wilmanns, W., 1999. Bcl-2: Bax and Bcl-xL expression in human sensitive and resistant leukemia cell lines. Leukemia 13, 1864–1872.

Orabi, K.Y., Abaza, M.S., Sayed, K.A.E., Elnagar, A.Y., Attiyah, R.A., Radhika, P.G., 2013. Selective growth inhibition of human malignant melanoma cells by syringic acid-derived proteasome inhibitors. Cancer Cell Int. 13, 82.

Quinn, B.A., Dash, R., Azab, B., Sarkar, S., Das, S.K., Kumar, S., Oyesanya, R.A., Dasgupta, S., Dent, P., Grant, S., Rahmani, M., Curiel, D.T., Dmitriev, I., Hedvat, M., Wei, J., Wu, B., Stebbins, J.L., Reed, J.C., Pellecchia, M., Sarkar, D., Fisher, P.B., 2011a. Targeting Mcl-1 for the therapy of cancer. Expert Opin. Investig. Drugs 20, 1397–1411.

Quinn, B.A., Dash, R., Azab, B., Sarkar, S., Das, S.K., Kumar, S., et al., 2011b. Targeting Mcl-1 for the therapy of cancer. Expert Opin. Investig. Drugs 20, 1397–1411.

Ramachandran, V., Raja, B., 2010. Protective effects of syringic acid against acetaminophen induced hepatic damage in albino rats. J. Basic Clin. Physiol. Pharmacol. 21, 369–385.

Reyna, D.E., Garner, T.P., Lopez, A., Kopp, F., Choudhary, G.S., Sridharan, A., Narayanagari, S.R., Mitchell, K., Dong, B., Bartholdy, B.A., Walensky, L.D., Verma, A., Steidl, U., Gavathiotis, E., 2017. Direct activation of BAX by BTSA1 overcomes apoptosis resistance in acute myeloid leukemia. Cancer Cell 32, 490–505.

Sawada, N., Nakashima, S., Banna, Y., Yamakawa, H., Hayashi, K., Takenaka, K., Nishimura, Y., Sakai, N., Nozawa, Y., 2000. Ordering of ceramide formation, caspase activation, and Bax/Bcl-2 expression during etoposide-induced apoptosis in C6 glioma cells. Cell Death Differ. 7, 761–772.

Schuettelkopf, A.W., Van Aalten, D.M.F., 2004. PRODRG: a tool for high-throughput crystallography of protein-ligand complexes. ActaCryst 60, 1355–1363.

Sharifi, S., Barar, J., Hejazi, M.S., Samadi, N., 2015. Doxorubicin changes bax/Bcl-xL ratio, caspase-8 and 9 in breast cancer cells. Adv. Pharm. Bull. 5 (3), 351–359.

Sippl, M.J., 1993. Recognition of errors in three-dimensional structures of proteins. Proteins 17 (4), 355–362.

Steiner, T., Koellner, G., 2001. Hydrogen bonds with p-acceptors in proteins: frequencies and role in stabilizing local 3-D structures. J. Mol. Biol. 305, 535–557.

Thompson, J.D., Higgins, D.G., Gibson, T.J., 1994. CLUSTAL W: improving the sensitivity of progressive multiple sequence alignment through sequence weighting, position-specific gap penalties and weight matrix choice. Nucleic Acids Res. 22, 4673–4680.

Tse, C., Shoemaker, A.R., Adickers, J., Chen, J., Jin, S., Johnson, E.F., et al., 2008. ABT-263: a potent and orally bioavailable Bcl-2 family inhibitor. Cancer Res. 68, 3421–3428.

Van Delft, M.F., Wei, A.H., Mason, K.D., Vandenberg, C.J., Chen, L., Czabotar, P.E., et al., 2006. The BH3 mimetic ABT-737 targets selective Bcl-2 proteins and efficiently induces apoptosis via Bak/Bax if Mcl-1 is neutralized. Cancer Cell 10, 389–399.

Vogler, M., Dinsdale, D., Dyer, M.J., Cohen, G.M., 2009. Bcl-2 inhibitors: small molecules with a big impact on cancer therapy. Cell Death Differ. 16, 360–367.

Walensky, L.D., Gavathiotis, E., 2011. BAX unleashed: the biochemical transformation of an inactive cytosolic monomer into a toxic mitochondrial pore. Trends Biochem. Sci. 36, 642–652.

Wang, G., Nikolovska-Coleska, Z., Yang, C.Y., Wang, R., Tang, G., Guo, J., Shangary, S., Qiu, S., Gao, W., Yang, D., Meagher, J., Stuckey, J., Krajewski, K., Jiang, S., Roller, P. P., Abaan, H.O., Tomita, Y., Wang, S., 2006. Structure-based design of potent small-molecule inhibitors of anti-apoptotic Bcl-2 proteins. J. Med. Chem. 49, 6139–6142.

Wei, J., Stebbins, J.L., Kitada, S., Sash, R., Zhai, D., Placzek, W.J., et al., 2011. An optically pure apogossypolone derivative as potent pan-active inhibitor of anti-apoptotic Bcl-2 family proteins. Front. Oncol. 1, 28.

Wilson, W.H., O'Connor, O.A., Czuczman, M.S., LaCasce, A.S., Gerecitano, J.F., Leonard, J.P., Tulpule, A., Dunleavy, K., Xiong, H., Chiu, Y.L., Cui, Y., Busman, T., Elmore, S. W., Rosenberg, S.H., Krivoshik, A.P., Enschede, S.H., Humerickhouse, R.A., 2010. Navitoclax, a targeted high-affinity inhibitor of Bcl-2, in lymphoid malignancies: a phase 1 dose-escalation study of safety, pharmacokinetics, pharmacodynamics, and antitumor activity. Lancet Oncol. 1, 1149–1159.

Xin, M., Li, R., Xie, M., Park, D., Owonikoko, T.K., Sica, G.L., Corsino, P.E., Zhou, J., Ding, C., White, M.A., Magis, A.T., Ramalingam, S.S., Curran, W.J., Khuri, F.R., Deng, X., 2014. Small-molecule Bax agonists for cancer therapy. Nat. Commun. 5, 4935.

Zhao, Y.H., Le, J., Abraham, M.H., Hersey, A., Eddershaw, P.J., Luscombe, C.N., Butina, D., Beck, G., Sherborne, B., Cooper, I., Platts, J.A., 2001. Evaluation of human intestinal absorption data and subsequent derivation of a quantitative structure-activity relationship (QSAR) with the Abraham descriptors. J. Pharm. Sci. 90, 749–784.

Zheng, Q., Wang, B., Gao, J., Xin, N., Wang, W., Song, X., Shao, Y., Zhao, C., 2018. CD155 knockdown promotes apoptosis via AKT/Bcl-2/Bax in colon cancer cells. J. Cell Mol. Med. 22, 131–140.

Zhu, L., Chen, Y., Wei, C., Yang, X., Cheng, J., Yang, Z., Chen, C., Ji, Z., 2018. Anti-proliferative and pro-apoptotic effects of cinobufagin on human breast cancer MCF-7 cells and its molecular mechanism. Nat. Prod. Res. 32, 493–497.